DOI: 10.1002/chem.200600207

# Electron Transfer in Nonpolar Solvents in Fullerodendrimers with Peripheral Ferrocene Units

**Laura Pérez,[a] Joaquín C. García-Martínez,[b] Enrique Díez-Barra,[b] Pedro Atienzar,[c] Hermenegildo García,[c] Julián Rodríguez-López,*[b] and Fernando Langa*[a]**

**Abstract:** Two new fullerodendrimers, with two and four ferrocene units on their periphery, have been synthesized by 1,3-dipolar cycloaddition reactions between the corresponding azomethine ylides and $C_{60}$. These new compounds have been studied by using cyclic voltammetry and UV/Vis spectroscopy. Weak intramolecular interactions between the fullerene cage and the ferrocene groups have been found. The photochemical events of both fullerene–ferrocene dendrimers have been probed by means of steady-state and time-resolved techniques. The steady-state emission intensities of the fulleropyrrolidine–ferrocene dendrimers **1** and **2** were found to be quenched relative to the *N*-methylfulleropyrrolidine without substituents that was used as a model. The nanosecond transient absorption spectral studies revealed efficient charge separation in both systems, even in toluene. The lifetimes of the $(C_{60})^{\bullet-}$–$(\text{dendron})^{\bullet+}$ are higher for the second-generation fullerodendrimer (with four ferrocene units) and they are of the order of tens of nanoseconds in toluene and hundreds of nanoseconds in polar solvents.

**Keywords:** dendrimers · donor–acceptor systems · electrochemistry · electron transfer · fullerenes

## Introduction

Photosynthesis, the process that converts solar into chemical energy, is essential for living organisms.[1] Light energy is absorbed by individual pigments, but is not used immediately by these pigments for energy conversion. Instead, the light energy is transferred to chlorophylls that are in a special protein environment in which the actual energy-conversion event occurs: the light energy is used to transfer an electron to a neighboring pigment. A large number of pigment molecules, collectively referred to as antenna, "harvest" light and transfer the light energy to the same reaction center.[2] The purpose is to maintain a high rate of electron transfer in the reaction center, even at lower light intensities. The complexity of photosynthesis prompts the use of simpler models, consisting of donor–acceptor-linked molecules, to get a better understanding of the process in order to be able to design and synthesize artificial systems that can efficiently process solar energy.[3] More recently, it has been recognized that artificial photosynthesis also has potential uses in molecular-scale optoelectronics, photonics, sensor design, and other areas of nanotechnology.[4]

Dendrimers have recently received a great deal of attention in the context of light-harvesting molecular antenna-type architectures[5] that mimic natural photosynthetic systems. In this respect, molecules in which an array of peripheral chromophores transfer the collected energy to a fullerene $C_{60}$ core have recently been described by several groups.[6] Thus, Nierengarten and Armaroli's groups have recently prepared fullerene-based dyads with oligophenylenevinylene (OPV) moieties and alkoxy groups in the periphery to reveal a very efficient OPV→$C_{60}$ photoinduced energy transfer.[7] We have synthesized fullerodendrimers in which a phenylenevinylene dendritic wedge is connected to the fullerene core through a pyrazoline ring and observed both energy and electron transfer from the excited antenna to the $C_{60}$ cage.[8] Related compounds have also been reported by

[a] Dr. L. Pérez, Dr. F. Langa
Facultad de Ciencias del Medio Ambiente
Universidad de Castilla-La Mancha, 45071 Toledo (Spain)
Fax: (+34) 925-268-840
E-mail: Fernando.LPuente@uclm.es

[b] Dr. J. C. García-Martínez, Dr. E. Díez-Barra, Dr. J. Rodríguez-López
Facultad de Química
Universidad de Castilla-La Mancha, 13071 Ciudad Real (Spain)
Fax: (+34) 926-295-318
E-mail: julian.rodriguez@uclm.es

[c] Dr. P. Atienzar, Dr. H. García
Instituto de Tecnología Química CSIC-UPV
Universidad Politécnica de Valencia, 46022 Valencia (Spain)

Supporting information ($^1$H and $^{13}$C NMR spectra for **1**–**4**) for this article is available on the WWW under http://www.chemeurj.org/ or from the author.

   

Martín, Guldi, and co-workers; in this case, either dibutylaniline or dodecyloxynaphthalene units on the periphery acted as antennas/electron donors and electron transfer was observed when using benzonitrile as the solvent.[9]

The modification of the properties of dendritic compounds by the introduction of metal atoms into their structure (metallodendrimers), especially those containing ferrocene, has attracted particular attention[10] due to the fact that ferrocene combines chemical versatility with high thermal stability. Moreover, ferrocene is an electron-transfer donor that is stronger than *N*,*N*-dimethylaniline or anisole[11] and several examples of efficient, photoinduced electron transfer in ferrocene–fullerene systems have been described.[12] Consequently, phenylenevinylene-based dendrimers with a fullerene core and peripheral ferrocene groups appear to be interesting systems for energy or electron transfer. With respect to the previously reported ferrocene–fullerene systems, our work has the novelty of using phenylenevinylene units as linkers. It is known that the connecting substructure between the donor and the acceptor of the dyad can influence the electron-acceptor ability of the fullerene core because it disrupts the spherical aromaticity of $C_{60}$. Thus, in this paper we report the synthesis, and electrochemical and photophysical properties of such fullerodendrimers in which two (**1**) and four (**2**) ferrocene electron donors are located at terminal positions.

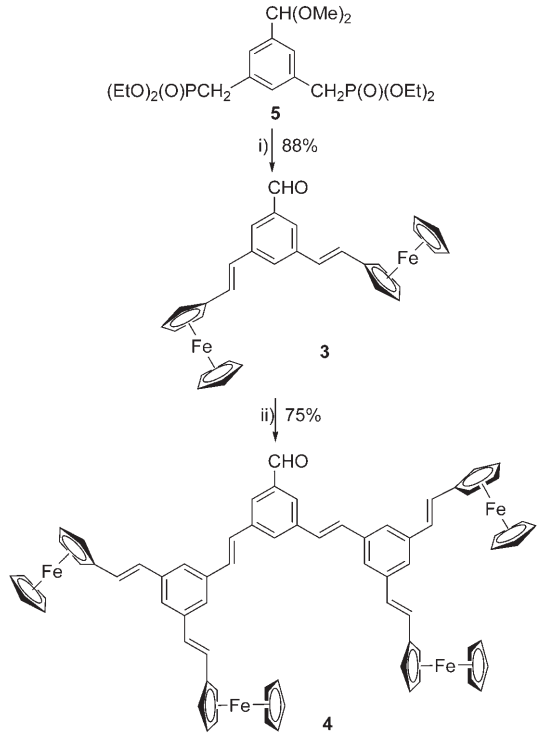


Scheme 1. Synthesis of ferrocene dendrons. Reagents and conditions: i) ferrocenecarboxaldehyde, *t*BuOK, THF; then $HCl/H_2O$; ii) **5**, *t*BuOK, THF; then $HCl/H_2O$.

## Results and Discussion

**Synthesis**: The synthesis of dendrons **3** and **4** was performed in a convergent manner by using the Horner–Wadsworth–Emmons (HWE) reaction between the diphosphonate derivative **5** and the appropriate aldehydes in *t*BuOK/THF (Scheme 1) following a methodology previously described by some of us.[13] Acid hydrolysis of the acetal groups gave **3**[14] and **4** in good yields (88 and 75%, respectively) as red solids. Mass spectrometry (MS) and NMR experiments (including distortionless enhancement by polarization transfer (DEPT)) confirmed the structures of the compounds (see the Experimental Section). The selectivity of the HWE reaction is sufficiently high to generate all-*trans* isomers within the limits of NMR detection. This stereochemistry for the double bonds was established by the coupling constant of the vinylic protons in the $^1$H NMR spectra ($J = 16$–$17$ Hz). High-resolution (HR) MS analyses gave the expected molecular ions.

The functionalization of $C_{60}$ was based on the 1,3-dipolar cycloaddition of the corresponding azomethine ylide,[15] generated in situ from aldehydes **3** and **4**, and *N*-methylglycine (sarcosine). The reaction of $C_{60}$ with **3** and **4** in the presence of excess *N*-methylglycine in toluene under reflux afforded pyrrolidinofullerenes **1** and **2** in 46 and 38% yield, respectively (Scheme 2). Fullerodendrimers **1** and **2** were purified by means of flash chromatography (toluene/hexane 8:2). The structural assignment of **1** and **2** was based on analytical and spectroscopic data (i.e., UV/Vis, FTIR, $^1$H NMR,

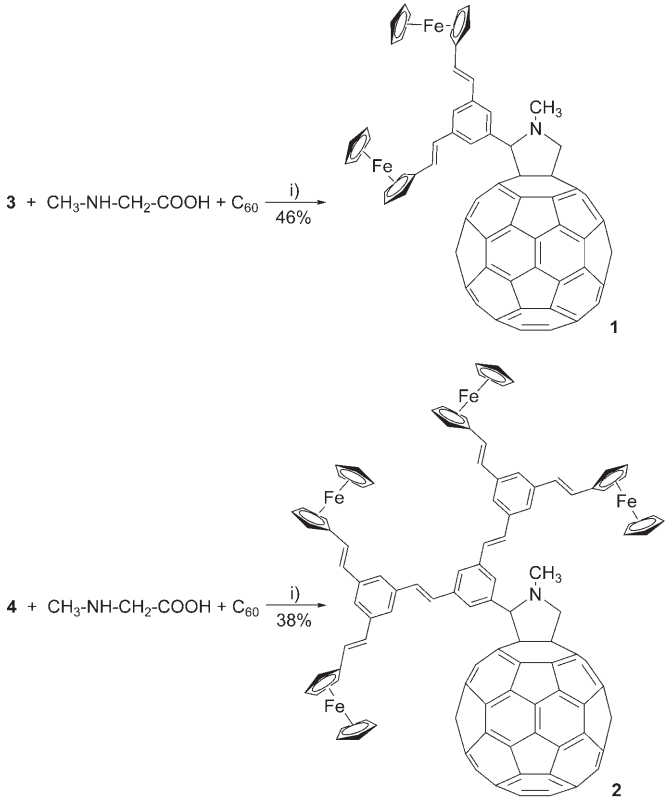


Scheme 2. Synthesis of fulleroferrocene dendrimers. Reagents and conditions: i) toluene/Δ.

  

$^{13}$C NMR, and MALDI mass spectra). The matrix-assisted laser desorption/ionization time-of-flight (MALDI-TOF) spectra showed peaks that matched the calculated values for the molecular weights. UV/Vis spectra revealed the typical dihydrofullerene absorption band at around $\lambda = 430$ nm. The $^1$H NMR spectra of **1** and **2** in $CDCl_3$ exhibit the expected features with the correct integration ratios. The signals of the pyrrolidine protons appeared as doublets ($J = 9.5$ Hz; geminal hydrogen atoms), and singlets in the $\delta = 4$–5 ppm zone, which is consistent with spectra obtained for similar derivatives.[16] The $^{13}$C NMR spectra contained the signals corresponding to the $sp^2$ and $sp^3$ atoms of $C_{60}$, and the expected signals corresponding to the organic addends.

**Electrochemistry**: The redox properties of the fulleroferrocene dendrimers were studied by using cyclic voltammetry (CV) at room temperature in $CH_2Cl_2$. The data obtained are summarized in Table 1. In the cathodic region, three quasi-reversible reduction waves were recorded, which correspond to the stepwise reduction of the fullerene cage (Figure 1).

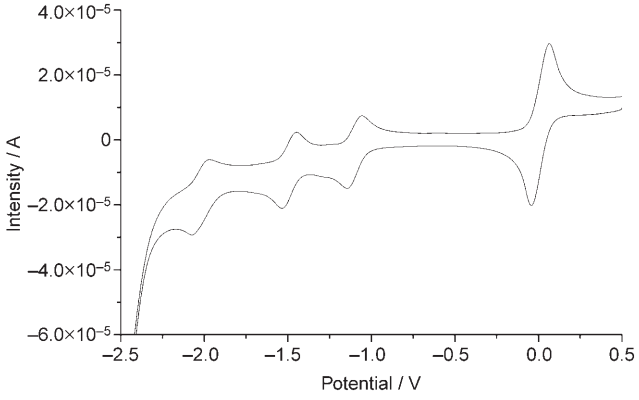


Figure 1. Cyclic voltammogram (scan rate 100 mV s$^{-1}$) of fulleroferrocene dendrimer **1** in $CH_2Cl_2$ at room temperature.

These reduction waves are slightly shifted to more negative potentials relative to those in the parent $C_{60}$. This behavior is a consequence of the saturation of a double bond on the $C_{60}$ cage in a similar way to other pyrrolidinofullerenes.[17]

In the anodic region, only a single reversible oxidation process corresponding to the ferrocene units was observed, which implies that the iron centers do not communicate with each other over the benzene bridge. Several facts can be inferred from Table 1: 1) aldehyde **3** is more difficult to oxidize than the parent ferrocene by 90 mV, whereas aldehyde **4** is easier to oxidize by 230 mV, thus indicating that the intramolecular electron-withdrawing effect of the CHO group is only effective in the first-generation compound owing to the conjugation not being extended by *meta* substitution; 2) analogous to system **4**, fullerodendrimers **1** and **2** are easier to oxidize than ferrocene as a consequence of the donating branches, and the oxidations become easier as the dendritic generation grows (from **3** to **4**, and from **1** to **2**) because of the larger electron-donating nature; and 3) more salient is the observation that the first-generation fullerodendrimer **1** is easier to oxidize than its precursor **3** by 170 mV reflecting the larger electron-withdrawing effect of the formyl group relative to the $C_{60}$–pyrrolidine group, however the second-generation compound **2** is more difficult to oxidize than **4** by 30 mV. It is not easy to explain the behavior of the second-generation fullerodendrimer **2** in terms of the nature of the substitution, as has recently been claimed for other ferrocene derivatives.[18] Although a possible explanation might be the existence of small electronic interactions[19] in **2** between the $C_{60}$ and the redox-active ferrocenyl moiety (see below), unequivocal evidence is still lacking and other possibilities cannot be neglected. The experimentally determined $HOMO_{(donor)}$–$LUMO_{(C_{60})}$ gap, calculated from the first oxidation and reduction potentials, is significantly lower for the second-generation fullerodendrimer **2** (0.99 eV) than that for the first-generation system **1** (1.11 eV).

**Steady-state absorption spectra**: The UV/Vis spectra of **3** and **4** in $CH_2Cl_2$ are shown in Figure 2. As one would expect, the *meta* arrangement through which the dendrons are linked causes the absorption spectra to consist essentially of a simple superposition of the absorptions due to the different phenylenevinylene chromophores. Indeed, the spectra are essentially dominated by strong bands with maxima at $\lambda = 314$–316 nm associated with these units. The absorptions become much stronger as the dendritic generation increases, a consequence of the exponential increase in the number of light-absorbing units. The $\lambda_{max}$ values are similar for both compounds (Table 1), showing that conjugation is not extended by *meta* substitution and, consequently, that these compounds behave respectively as an assembly of two and four vinylferrocene moieties sharing a phenyl ring. The value of $\varepsilon$, compared with that of *N*-methylfulleropyrrolidine

Table 1. Selected UV/Vis, photoluminescence (PL), and electrochemical data[a] of ferrocene, compounds **1**–**4**, and $C_{60}$.

| | $E_{ox}$ [V] | $E^1_{red}$ [V] | $E^2_{red}$ [V] | $E^3_{red}$ [V] | UV/Vis[b] $\lambda_{max}$ [nm] ($\varepsilon$, [M$^{-1}$cm$^{-1}$]) | PL[c] $\lambda_{max}$ [nm] | $\Phi_f$[d] |
|---|---|---|---|---|---|---|---|
| ferrocene | +0.11 | – | – | – | | | |
| **3** | +0.20 | – | – | – | 249 (35600), 314 (39600), 456 (3900) | 421 | $1.2\times10^{-3}$ |
| **4** | −0.12 | – | – | – | 259 (59100), 316 (116400), 462 (4200) | 421 | $1.3\times10^{-3}$ |
| **1** | +0.03 | −1.08 | −1.48 | −2.03 | 256 (151500), 315 (85500), 431 (7050) | 423 | $3.45\times10^{-4}$ |
| **2** | −0.09 | −1.08 | −1.47 | −1.99 | 257 (203600), 318 (172600), 431 (8860) | 422 | $3.96\times10^{-4}$ |
| $C_{60}$ | – | −0.97 | −1.36 | −2.03 | | | |

[a] Calculated as averages of $E_{ox}$ and $E_{red}$. See the Experimental Section for CV details. [b] All spectra were recorded in $CH_2Cl_2$ (**3** and **4**: $c = 3\times10^{-6}$ M; **1** and **2**: $c = 5\times10^{-6}$ M) at RT. [c] All spectra were recorded in toluene at RT; $\lambda_{exc} = 323$ nm. [d] Determined by using $C_{60}$ as the standard ($\Phi_f = 3.2\times10^{-4}$).[28]

  

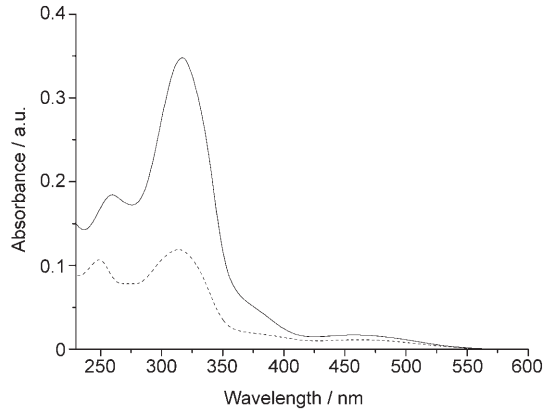


Figure 2. UV/Vis spectra of **3** (-----) and **4** (——) in $CH_2Cl_2$ ($c=3\times10^{-6}$ M) at room temperature.

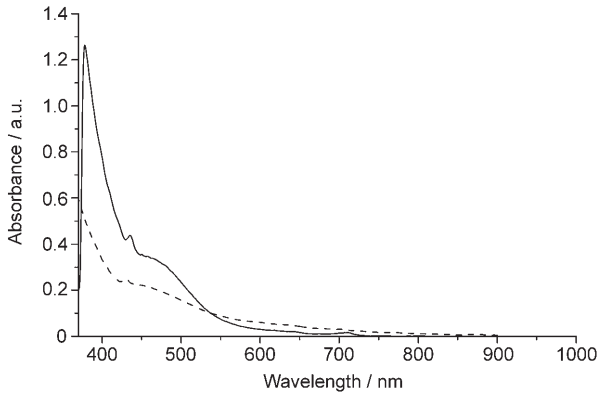


Figure 4. UV/Vis spectra of **2** in cyclohexane (-----) and in carbon disulfide (——) ($c=5\times10^{-5}$ M) at room temperature.

($\varepsilon=22200$ at 326 nm), shows the light-harvesting ability of these fullerodendrimers. A broad band in the visible region ($\lambda=420$–550 nm) that is characteristic of the metal-centered d–d absorption of ferrocene derivatives was also observed.

The absorption spectra of the pyrrolidino[60]fullerene dendrimers **1** and **2** were also measured in $CH_2Cl_2$ (Figure 3, Table 1). The spectra of both **1** and **2** display two very intense bands in the UV region and much weaker features in the visible spectral region (Figure 3, inset). The band maxima at $\lambda_{max}=256$ (**1**) and 257 nm (**2**), and the lowest allowed singlet transitions at $\lambda_{max}=431$ nm are characteristic absorptions of a fullerenepyrrolidine. The shapes of the broad bands in the visible region are different to those of precursors **3** and **4**, a fact that supports the presence of modest interactions in the ground state between the ferrocene groups and the fullerene cage.[20,21] The intensity of this broad band for compound **2** was enhanced in the more polar solvent carbon disulfide and remained as such when cyclohexane was used as the solvent (Figure 4).[22]

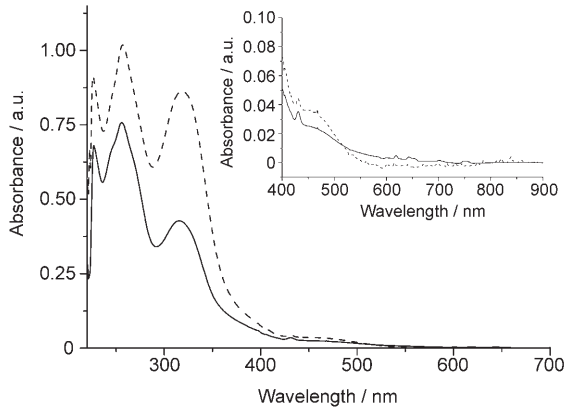


Figure 3. UV/Vis spectra of **1** (——) and **2** (-----) in $CH_2Cl_2$ ($c=5\times10^{-6}$ M) at room temperature.

**Steady-state fluorescence**: The excited-state properties of donor–bridge–acceptor systems are sensitive measures for proving intramolecular transfer dynamics and we have studied them in our dendrimer-functionalized fullerene derivatives **1** and **2**. The fluorescence spectra of ferrocenyl dendrimers **3** and **4** in toluene at room temperature and excited at 323 nm (where most of the incident light is absorbed by the phenylenevinylene moieties, $\lambda_{max}$ in toluene for **3**) are reported in Figure 5; this shows maxima at 421 nm with quantum yields ($\Phi_f$) of $1.2\times10^{-3}$ and $1.3\times10^{-3}$, respectively. In fullerodendrimers **1** and **2**, this emission is strongly quenched with $\Phi_f=3.45\times10^{-4}$ for **1** and $3.96\times10^{-4}$ for **2** (Table 1), indicating the occurrence of excited-state processes (energy or electron transfer) from the singlet excited state of the dendrimer.

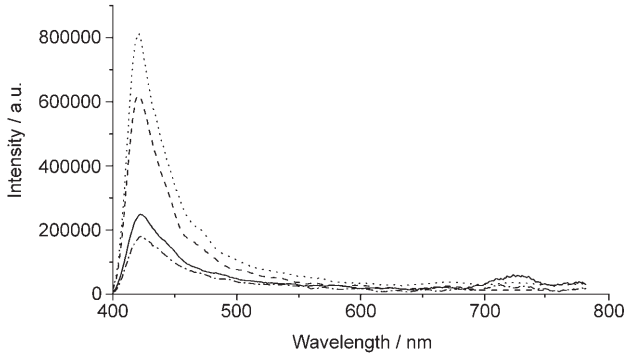


Figure 5. Fluorescence spectra of **1** (-•--•-), **2** (——), **3** (– – –), and **4** (-----) in toluene at matched absorptions ($\lambda_{exc}=323$ nm).

On monitoring the wavelength region of fulleropyrrolidine emission[23] (650–750 nm) upon excitation of the fullerene moiety, a very weak emission was found in the case of **2** and no emission was found in **1** (Figure 6). The emission of the model *N*-methylfulleropyrrolidine **5** is shown for comparison, being by far the strongest fluorescence intensity. The weak emission observed for **2** (upon excitation of the fullerene chromophore at 430 nm) in toluene was totally

  

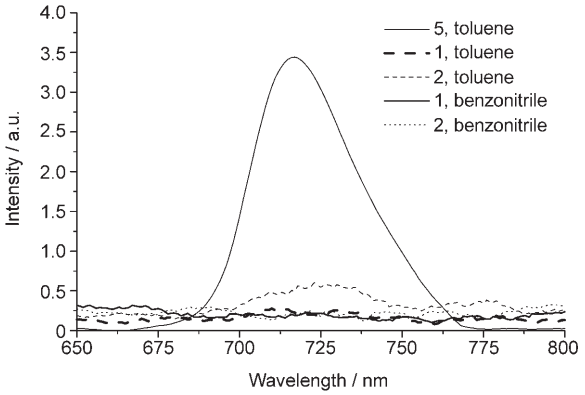


Figure 6. Emission spectra (fullerene region, $\lambda_{ex}=430$ nm) of compounds **1** and **2** in different solvents at matched absorptions. We have also included the emission of *N*-methylfulleropyrrolidine **5** for comparison.

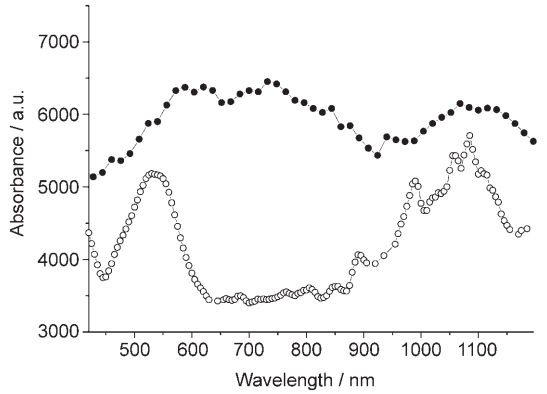


Figure 7. Transient absorption spectra of **1** in deoxygenated toluene (●) and in deoxygenated benzonitrile (○) recorded 2 μs after excitation with a nanosecond laser (excitation at 355 nm).

quenched when the more polar solvent benzonitrile was used. Although the dendritic component of **2** also absorbs at 430 nm and the fullerene emission decrease can be partially due to the filter effect of the dendron over the fullerene absorption, it is the different behavior from toluene to benzonitrile (in both solvents the filter effect should remain constant) that supports a polarity-dependent quenching of fullerene emission by the dendron. These facts suggest that the fullerene emission is quenched in benzonitrile by the dendrons, most probably through an electron-transfer process from the electron-donating ferrocenyl dendritic wedge to the fullerene cage to form a charge-separated state.

**Transient absorption studies**: To verify the quenching mechanism and characterize the reaction products, nanosecond transient absorption studies in toluene, acetonitrile, and benzonitrile were performed. Transient absorption spectra of fullerodendrimers in toluene were found in general to be broader than those recorded in benzonitrile, and had ill-defined peaks. On irradiation with a 355 nm laser in deoxygenated toluene, the generation of other transients or energy transfer (the absorption at 700 nm may correspond to the $C_{60}$ triplet excited state[24]), in addition to photoinduced electron transfer, can take place. In a more polar solvent such as benzonitrile, the photoinduced electron transfer is the prevalent process, as indicated by the observation of the band between 900–1200 nm for **1** (Figure 7), which is a clear attribute of the monofunctionalized fullerene radical anion.[25] The extinction coefficient of the ferricenium cation (formed concomitantly with the fullerene radical anion) was too small to be detected.[26]

The same behavior was observed for the second-generation ferrocene fullerodendrimer **2**. A broad transient absorption in toluene, probably encompassing different transients arising from energy and electron transfer, and a more-defined band at 900–1200 nm in benzonitrile, attributable to the radical anion centered at the fullerene moiety, were obtained (Figure 8).

On the other hand, when a solution of **2** in benzonitrile was irradiated in the presence of oxygen, the absorption

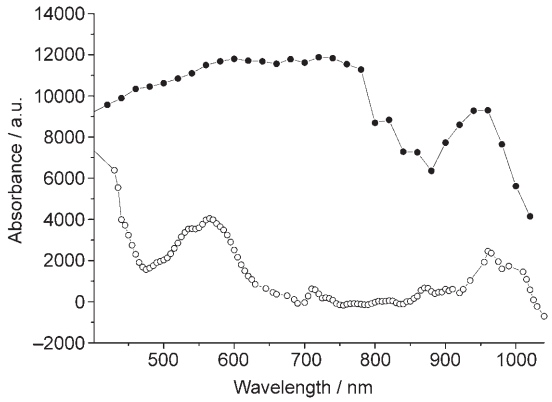


Figure 8. Nanosecond transient absorption spectra of **2** in deoxygenated toluene (●) and in deoxygenated benzonitrile (○) recorded 2 μs after excitation with a nanosecond laser (excitation at 355 nm).

band corresponding to the fullerene anion radical was quenched. It has been reported that the radical-ion pair in fullerene dyads reacts with molecular oxygen.[27]

Rate constants for both systems **1** and **2** in polar and nonpolar solvents (see Table 2) have been estimated from temporal profiles (Figure 9; $k_{CR}$ from the decay of the charge-separation excited state and $k_T$ from the decay of the triplet excited state). Generation of the charge-separated state is completed in the first nanoseconds after the laser flash. Thus, using our nanosecond laser flash photolysis system, formation of the charge-separated state instantaneously oc-

Table 2. Rate constants for charge-recombination ($k_{CR}$) and triplet-decay rate constants ($k_T$) of fullerodendrimers **1** and **2** in deaerated toluene, benzonitrile, and acetonitrile.

| | Solvent | $k_{CR}$ [$s^{-1}$] | $k_T$ [$s^{-1}$] |
|---|---|---|---|
| **1** | toluene | $2.50\times10^7$ | $8.47\times10^8$ |
| | benzonitrile | $1.78\times10^7$ | – |
| | acetonitrile | $8.47\times10^7$ | $1.23\times10^9$ |
| **2** | toluene | $1.35\times10^7$ | $8.62\times10^8$ |
| | benzonitrile | $9.70\times10^6$ | – |
| | acetonitrile | $6.99\times10^6$ | $1.33\times10^9$ |

  

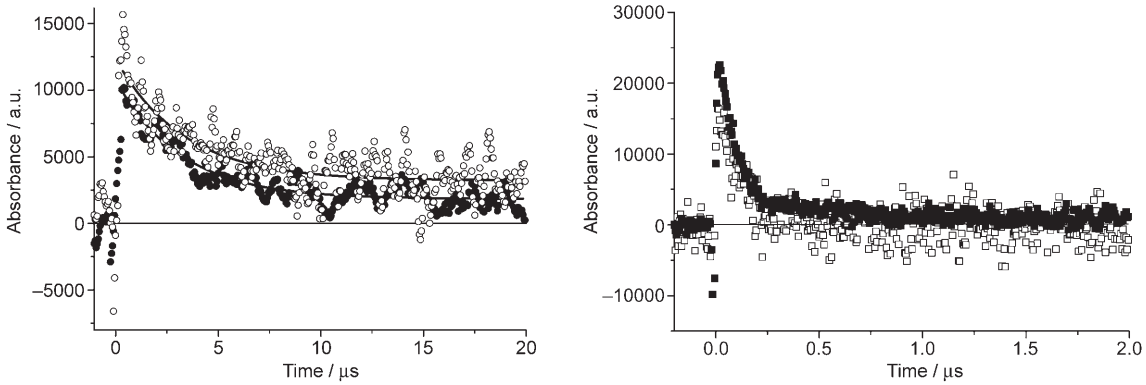


Figure 9. Temporal signal profiles monitored at 1000 nm of dyad **1** (○/□) and dyad **2** (●/■) in deaerated benzonitrile (left) and in oxygen-purged benzonitrile (right).

curred during the laser pulse and, therefore, $k_{CS}$ must be higher than $10^9\ s^{-1}$ for fullerodendrimers **1** and **2**. It should be remarked that in both dyads, in polar and nonpolar solvents, the deactivation constant of $^3C_{60}$* ($k_T$) is higher than that previously observed for *N*-methylfulleropyrrolidine, used as the reference ($k_T = 4.1\times10^4\ s^{-1}$ in benzene), which suggests the occurrence of paths for deactivation[28] other that the deactivation to the ground state by phosphorescence (see below).

The quantum yields for charge separation ($\Phi_{CS}$) were calculated according to Equation (2) from the fluorescence lifetimes for **1** and **2** [$\tau_{dyad}$, estimated according to Eq. (1)] by using *N*-methylfulleropyrrolidine as the reference ($\tau_{ref}$ = 1.3 ns);[29] $k_0$ is the fluorescence decay rate of the reference.[30] These values are collected in Table 3 together with the lifetimes of fluorescence and the radical-ion pair as calculated from time profiles.

$$k_{CS} = \frac{1}{\tau_{dyad}} - \frac{1}{\tau_{ref}} \quad (1)$$

$$\Phi_{CS} = \frac{[(1/\tau_{dyad}) - (1/\tau_{ref})]}{(1/\tau_{dyad})} = \frac{k_{CS}}{(k_{CS} + k_0)} \quad (2)$$

Table 3 shows that in all of the studied solvents the lifetimes of the charge-separated state of **2** are higher than those of **1**, as expected, due to the longer distance between the donor and acceptor moieties in **2**. It should be noted that the radical-ion pair is formed in both fullerodendrimers **1** and **2** in toluene with lifetimes of several tens of nanoseconds. Lifetimes are increased by a factor of 2–3 in polar solvents, and are as long as 143 ns for **2** in acetonitrile.

Table 3. Radical-ion-pair lifetimes ($\tau_{IP}$), fluorescence lifetimes ($\tau_{dyad}$), and quantum yields for charge separation ($\Phi_{CS}$) for compounds **1** and **2** in different solvents.

| | Solvent | $\tau_{IP}$ [ns][a] | $\tau_{dyad}$ [ns][b] | $\Phi_{CS}$ |
|---|---|---|---|---|
| **1** | toluene | 40 | 1.18 | 0.092 |
| | benzonitrile | 56 | 0.95 | 0.269 |
| | acetonitrile | 118 | 0.81 | 0.377 |
| **2** | toluene | 74 | 1.16 | 0.108 |
| | benzonitrile | 103 | 0.83 | 0.362 |
| | acetonitrile | 143 | 0.75 | 0.423 |

[a] Calculated from time profiles. [b] Calculated from time profiles by using Equation (1).

In contrast to related fullerodendrimers with peripheral dimethylanilino units,[9] which show only energy transfer in toluene, and electron transfer in benzonitrile, the systems presented here show electron transfer in both solvents. Moreover, in benzonitrile, the measured quantum yields for charge separation ($\Phi_{CS}$) are 0.269 for **1** and 0.362 for **2**, significantly higher than those reported for fullerodendrimers with dimethylanilino peripheral units ($\Phi \approx 0.1$). Nevertheless, our quantum yield values for charge separation are lower than previously reported data for related fullerene–ferrocene dyads in polar solvents, although in these cases the lifetimes of the charge-separated states were much shorter than those described here (56–103 ns) under similar conditions.[29] On the other hand, Guldi and co-workers reported longer lifetimes for fullerene charge-separated states (360–725 ns) than those measured by us.[9]

**Energetics of charge separation and charge recombination**: The energetics of the charge-separation and charge-recombination processes in systems **1** and **2** were evaluated to assess the feasibility of the electron-transfer process between the ferrocene units and $C_{60}$ in the excited state. The free-energy changes of the charge-recombination process ($\Delta G_{CR}$) were calculated by using the continuous dielectric model [Eq. (3)] from the first $E_{red}$ and $E_{ox}$ values.

$$-\Delta G_{CR} = E_{ox}(D) - E_{red}(C_{60}) + \Delta G_S \quad (3)$$

Here, $E_{ox}(D)$ and $E_{red}(C_{60})$ are the oxidation and reduction potentials of the donor and acceptor moieties, respectively, and $\Delta G_S$ refers to the static energy that is calculated according to Equation (4):[31]

$$\Delta G_S = \frac{e^2}{4\pi\varepsilon_0}\left(\frac{1}{2R_+} + \frac{1}{2R_-} - \frac{1}{R_{cc}}\right)\frac{1}{\varepsilon_S} - \frac{e^2}{4\pi\varepsilon_0}\left(\frac{1}{2R_+} + \frac{1}{2R_-}\right)\frac{1}{\varepsilon_T} \quad (4)$$

  

In this equation, $e$ is the electron charge, $\varepsilon_0$ is the vacuum permittivity, $\varepsilon_S$ is the static dielectric constant of the solvent used for rate measurements, and $\varepsilon_T$ is static dielectric constant of the solvent used for redox potential measurements. $R_+$ (**1**: $R_+ = 5.31$ Å; **2**: $R_+ = 7.65$ Å) and $R_-$ (4.4 Å) are the radii of the donor and acceptor, respectively; $R_{cc}$ is the center-to-center distance between the ions measured by molecular-mechanics calculations (**1**: $R_{cc} = 12.33$ Å; **2**: $R_{cc} = 14.67$ Å).[32]

From $\Delta G_{CR}$, the free-energy changes of the charge-separation process ($\Delta G_{CS}$) were calculated according to Equation (5) where $\Delta E_{00}$ (1.762 eV) is the excited-state energy from which the electron transfer occurs.[33] The results are given in Table 4.

$$-\Delta G_{CS} = \Delta E_{00} - (-\Delta G_{CR}) \quad (5)$$

The charge-separated states are significantly lower in energy in polar solvents (0.91–0.95 eV), and even in nonpolar solvents (1.55–1.62 eV), than those of fullerene singlet excited states (1.76 eV) suggesting that electron transfer is energetically feasible for both dyads.

Table 4. Free-energy changes and thermodynamic parameters ($\lambda$, $\Delta G^{\neq}$; both in eV) for intramolecular electron-transfer events in fullerene-based compounds **1** and **2**.

| | Solvent | $\varepsilon_{solvent}$ | $\Delta G_S$ | $-\Delta G_{CR}$ | $-\Delta G_{CS}$ | $\lambda$ | $\lambda_e$ | $\Delta G^{\neq}$ |
|---|---|---|---|---|---|---|---|---|
| **1** | toluene | 2.38 | 0.43 | 1.62 | 0.14 | 0.35 | 0.05 | 0.032 |
| | benzonitrile | 25.2 | −0.26 | 0.93 | 0.83 | 1.01 | 0.71 | 0.008 |
| | acetonitrile | 35.94 | −0.28 | 0.91 | 0.85 | 1.26 | 0.96 | 0.033 |
| **2** | toluene | 2.38 | 0.38 | 1.55 | 0.21 | 0.34 | 0.044 | 0.013 |
| | benzonitrile | 25.2 | −0.23 | 0.95 | 0.82 | 0.92 | 0.62 | 0.003 |
| | acetonitrile | 35.94 | −0.24 | 0.93 | 0.83 | 1.14 | 0.84 | 0.021 |

The total reorganization energy ($\lambda$) is the sum of the internal term, $\lambda_i$, and the external reorganization energy term, $\lambda_e$, and is solvent dependent. In fullerene derivatives, $\lambda_i$ has a value of 0.3 eV[23] and $\lambda_e$ was estimated from Equation (6) in which $n$ is the solvent refractive index.

$$\lambda_e = \frac{e^2}{4\pi\varepsilon_0}\left[\frac{1}{2}\left(\frac{1}{R_+}+\frac{1}{R_-}\right)-\frac{1}{R_{cc}}\right]\left(\frac{1}{n^2}-\frac{1}{\varepsilon_S}\right) \quad (6)$$

From these data the activation energy barrier ($\Delta G^{\neq}$) for charge separation was calculated by using Equation (7). The data are summarized in Table 4.

$$\Delta G^{\neq} = \frac{(\Delta G_{CS}+\lambda)^2}{4\lambda} \quad (7)$$

According to the Marcus theory of electron transfer,[34] the electronic coupling and the reorganization energy ($\lambda$) regulate the rate constants for charge separation and charge reorganization. Under optimal conditions, small reorganization energies lead to optimal charge-separation kinetics and a deceleration of the charge-recombination rates.[35] Table 4 shows that the photoinduced charge-separation process is in the "normal" Marcus region because $\Delta G_{CS} > -\lambda$, irrespective of the solvent or the generation of the dendritic donor. It should be remarked that the low value of $\lambda$ in toluene ($\lambda \approx 0.3$ eV) is similar to that observed in natural systems.

The energy diagrams in polar and nonpolar solvents can be illustrated as shown in Figure 10 for ferrocene–dendrimer–fullerene (Fc–dn–$C_{60}$) **2**. The energy level of $^1(Fc_4–dn_2)^*–C_{60}$ was evaluated to be 2.94 eV from fluorescence data. The energy levels of $^1C_{60}^*$ and $^3C_{60}^*$ (1.76 eV and 1.50 eV) were reported in the literature,[33,36] and the radical-ion-pair energy levels were calculated from Equation (3) and are dependent on the solvent polarity. Excitation at 355 nm should form $^1(Fc_4–dn_2)^*–C_{60}$ (2.94 eV), which through an energy-transfer (EnT) process forms $(Fc_4–dn_2)–^1C_{60}^*$; then an intersystem crossing (ISC) to $(Fc_4–dn_2)–^3C_{60}^*$ ($\approx 1.50$ eV) occurs, competing in toluene with an electron-transfer (ET) process to form the radical-ion pair ($\approx 1.55$ eV), and an equilibrium between both species should exist as indicated above. Finally, the CS state decays to the ground state by a charge-recombination process. In benzonitrile or acetonitrile, a similar energy diagram can be depicted. In these cases, as a consequence of the higher stability of the radical-ion pair (0.95 eV in benzonitrile, 0.93 eV in acetonitrile) due to the higher polarity of the solvent, CS takes place quite efficiently as confirmed by time-resolved fluorescence experiments.

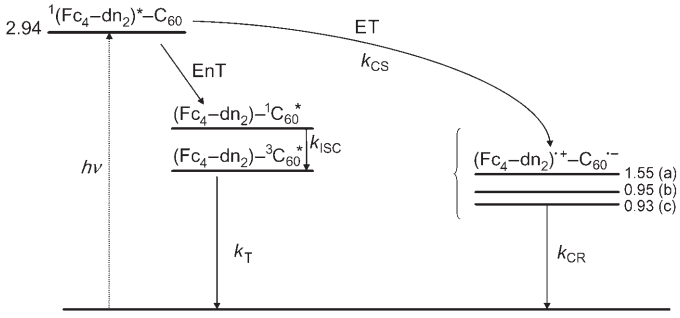


Figure 10. Schematic energy diagrams for charge-separation and charge-recombination processes in dyad **2** in a) toluene, b) benzonitrile, and c) acetonitrile. Numbers indicate energy levels in eV relative to the ground state.

## Conclusion

The synthesis of new $C_{60}$-based dendrimers **1** and **2** with two or four ferrocene units, respectively, as donors located on the periphery has been accomplished by means of a new convergent route. Cyclic voltammetry studies indicated an

  

electrochemically determined HOMO–LUMO gap as low as 0.99 eV for the second-generation fullerodendrimer **2**. UV/Vis spectra show similar $\lambda_{max}$ for both fullerodendrimers **1** and **2** suggesting that these compounds behave as an assembly of two and four vinylferrocene moieties, respectively. The appearance of a broad band between 450 and 500 nm, enhanced in more polar solvents, suggests the existence of weak ground-state interactions between the vinylferrocene moieties and the fullerene sphere. Photophysical investigations show an efficient photoinduced electron-transfer process even in toluene, with higher quantum yields as the dendrimer generation is increased. The lifetimes of the charge-separated state vary from tens of nanoseconds in nonpolar solvents to hundreds of nanoseconds in polar solvents, with a higher value for the second-generation fullerodendrimer **2** due to the longer distance between the ferrocene and the $C_{60}$ cage.

## Experimental Section

General experimental conditions have been reported previously.[13] NMR spectra were recorded in $CDCl_3$. Chemical shifts are given in ppm relative to tetramethylsilane (TMS) ($^1$H, 0.0 ppm) or $CDCl_3$ ($^{13}$C, 76.9 ppm). Cyclic voltammetry measurements were carried out on an Autolab PGSTAT 30 potentiostat using a BAS MF-2062 reference electrode (Ag/0.01 M $AgNO_3$; 0.1 M $n$Bu$_4$NClO$_4$ in acetonitrile), an auxiliary electrode consisting of a Pt wire, and a Metrohm 6.1247.000 conventional glassy carbon electrode (3 mm o.d.) as a working electrode directly immersed in the solution. A 10 mL electrochemical cell from BAS, Model VC-2, was also used. The experiments were carried out with a scan rate of 100 mV s$^{-1}$ in dry $CH_2Cl_2$ (0.1 M $n$Bu$_4$NClO$_4$) at RT. All commercially available compounds were used without further purification. $C_{60}$ was purchased from MER Corporation (Tucson, AZ). Diphosphonate derivative **5** was prepared according to a procedure previously reported by some of us.[13]

The time-resolved fluorescence spectra were measured at RT in $N_2$-purged sealed quartz cells using an Edinburgh FL3000 spectrofluorimeter with a Xe-doped mercury lamp and a Czerny–Turner monochromator.

Laser flash photolysis experiments were carried out by using the third (355 nm) harmonic of a Q-switched Nd:YAG laser (Spectron Laser Systems, UK; pulse width ca. 9 ns and 35 mJ pulse$^{-1}$). The signal from the monochromator/photomultiplier detection system was captured by using a Tektronix TDS640 A digitizer and transferred to a PC computer that controlled the experiment and provided suitable processing and data-storage capabilities. Fundamentals and details of similar time-resolved laser setups have been published elsewhere.

**General procedure for the Horner–Wadsworth–Emmons reaction**: All glassware was oven-dried and cooled under argon. Potassium *tert*-butoxide (3 mmol) was added, in small portions, to a stirred solution of diphosphonate **5** (1 mmol) and the corresponding aldehyde (2 mmol) in THF (100 mL), under argon. The dark-red mixture was stirred for the indicated period of time at RT. After hydrolysis with 1 M HCl (50 mL), the mixture was stirred for an additional 3 h at RT in order to remove the acetal group. It was then carefully neutralized with 1 M NaOH, extracted with $CHCl_3$ (×3), and dried ($MgSO_4$). The solution was filtered and the solvent was evaporated under reduced pressure. The crude product was purified by using column chromatography (silica gel, hexanes/$CH_2Cl_2$ 4:6).

**Dendron 3**: Reaction time: 1 h; red solid; yield: 88%; $^1$H NMR (300 MHz, $CDCl_3$): $\delta$ = 4.16 (s, 10H), 4.34 (t, $J$ = 1.5 Hz, 4H), 4.51 (t, $J$ = 1.5 Hz, 4H), 6.75 (A of AB$_q$, $J$ = 16.5 Hz, 2H), 7.03 (B of AB$_q$, $J$ = 16.2 Hz, 2H), 7.66 (brs, 1H), 7.80 (d, $J$ = 1.5 Hz, 2H,), 10.06 ppm (s, 1H); $^{13}$C NMR and DEPT (75 MHz, $CDCl_3$): $\delta$ = 67.1 (CH), 69.3 (CH), 69.4 (CH), 82.6 (C), 124.4 (CH), 124.7 (CH), 129.0 (CH), 129.2 (CH), 137.2 (C), 139.2 (C), 192.6 ppm (CHO); IR (KBr): $\tilde{\nu}$ = 1694 cm$^{-1}$; MS (EI): $m/z$ (%): 527 (48) [$M^+$+1], 526 (100) [$M^+$]; HRMS: $m/z$ calcd for $C_{31}H_{26}O_{56}Fe_2O$: 526.0682; found: 526.0678.

**Dendron 4**: Reaction time: 2 h; red solid; yield: 75%; $^1$H NMR (300 MHz, $CDCl_3$): $\delta$ = 4.17 (s, 20H), 4.30 (t, $J$ = 1.5 Hz, 8H), 4.50 (t, $J$ = 1.5 Hz, 8H), 6.76 (A of AB$_q$, $J$ = 16.2 Hz, 4H), 6.97 (B of AB$_q$, $J$ = 16.2 Hz, 4H), 7.24 (A of AB$_q$, $J$ = 16.5 Hz, 2H), 7.31 (B of AB$_q$, $J$ = 16.2 Hz, 2H), 7.40 (brs, 2H), 7.48 (brs, 4H), 7.89 (brs, 1H), 7.94 (brs, 2H), 10.10 ppm (s, 1H); $^{13}$C NMR and DEPT (75 MHz, $CDCl_3$): $\delta$ = 67.0 (CH), 69.2 (CH), 69.3 (CH), 83.1 (C), 122.5 (CH), 123.2 (CH), 125.6 (CH), 126.4 (CH), 127.3 (CH), 127.7 (CH), 130.1 (CH), 130.7 (CH), 137.3 (C), 137.3 (C), 138.7 (C), 138.8 (C), 192.2 ppm (CHO); IR (KBr): $\tilde{\nu}$ = 1697 cm$^{-1}$; MS (FAB$^+$): $m/z$ (%): 1151 (11) [$M^+$+1], 1150 (11) [$M^+$]; HRMS: $m/z$ calcd for $C_{71}H_{58}Fe_4O$: 1150.1885; found: 1150.1883.

**General procedure for the synthesis of pyrrolidino[60]fullerenes 1 and 2**: A solution of $C_{60}$ (0.038 mmol), the corresponding aldehyde (0.038 mmol), and *N*-methylglycine (0.19 mmol) in toluene (40 mL) was heated under reflux under an argon atmosphere for the indicated period of time. The solvent was evaporated and the crude material was purified by using flash chromatography on silica gel using toluene/hexane (8:2) as the eluent. Further purification of the solid was accomplished by centrifugation (×3) with methanol and *n*-pentane.

**Fullerodendrimer 1**: Reaction time: 17 h; yield: 46% (60% based on reacted $C_{60}$); $^1$H NMR (400 MHz, $CDCl_3$): $\delta$ = 2.93 (s, 3H), 4.14 (s, 10H), 4.29 (t, $J$ = 1.5 Hz, 4H), 4.31 (d, $J$ = 9.5 Hz, 1H), 4.50 (t, $J$ = 1.5 Hz, 4H), 4.95 (s, 1H), 5.04 (d, $J$ = 9.5 Hz, 1H), 6.74 (A of AB$_q$, $J$ = 16.3 Hz, 2H), 6.94 (B of AB$_q$, $J$ = 16.3 Hz, 2H), 7.18 (brs, 2H), 7.44 ppm (brs, 1H); $^{13}$C NMR (50 MHz, $CDCl_3$): $\delta$ = 40.4, 67.0, 67.4, 69.2, 69.4, 69.5, 70.3, 83.2, 83.7, 123.4, 124.9, 125.0, 125.2, 125.6, 127.7, 128.1, 128.7, 135.6, 136.4, 137.5, 138.4, 139.5, 139.8, 140.1, 141.6, 141.8, 142.0, 142.1, 142.4, 143.0, 144.2, 144.4, 144.9, 145.1, 145.2, 145.3, 145.4, 145.5, 145.75, 145.83, 145.96, 146.0, 146.5, 147.1, 153.2, 153.8, 155.9 ppm; IR (KBr): $\tilde{\nu}$ = 1553, 532 cm$^{-1}$; UV/Vis ($CH_2Cl_2$): $\lambda_{max}$ (log $\varepsilon$) = 256 (5.19), 315 (4.94), 430 nm (4.12); MALDI-TOF MS: $m/z$: 1273.2 [$M^+$], 720 [$C_{60}$].

**Fullerodendrimer 2**: Reaction time: 7 h; yield: 38% (60% based on reacted $C_{60}$); $^1$H NMR (200 MHz, $CDCl_3$): $\delta$ = 2.92 (s, 3H), 4.17 (s, 20H), 4.31 (t, $J$ = 1.7 Hz, 8H), 4.33 (d, $J$ = 9.5 Hz, 1H), 4.50 (t, $J$ = 1.7 Hz, 8H), 5.01 (s, 1H), 5.07 (d, $J$ = 9.5 Hz, 1H), 6.75 (A of AB$_q$, $J$ = 16.1 Hz, 4H), 6.98 (B of AB$_q$, $J$ = 16.1 Hz, 4H), 7.26 (brs, 4H), 7.38 (s, 2H), 7.50 (brs, 5H), 7.75 ppm (s, 1H); $^{13}$C NMR (50 MHz, $CDCl_3$): $\delta$ = 40.6, 67.2, 69.3, 69.5, 69.7, 70.3, 83.3, 83.7, 122.7, 123.3, 124.7, 126.0, 127.3, 127.8, 129.3, 130.0, 135.7, 135.9, 136.5, 136.7, 137.7, 137.9, 138.5, 139.6, 140.0, 140.1, 141.56, 141.64, 142.0, 142.1, 142.2, 142.5, 143.0, 144.3, 144.5, 145.2, 145.3, 145.4, 145.5, 145.7, 145.9, 146.1, 146.2, 146.4, 146.6, 146.6, 147.2, 153.2, 153.3, 153.9, 156.0 ppm; IR (KBr): $\tilde{\nu}$ = 1531, 625, 528 cm$^{-1}$; UV/Vis ($CH_2Cl_2$): $\lambda_{max}$ (log $\varepsilon$) = 257 (5.31), 318 (5.24), 430 nm (3.90); MALDI-TOF MS: $m/z$: 1896.8 [$M^+$].

## Acknowledgements

Financial support for this work was provided by a grant from the Ministerio de Educación y Ciencia of Spain and FEDER funds (projects CTQ2004-00364/BQU and BQU-2002-01327) and the Junta de Comunidades de Castilla-La Mancha (projects PAI-05-068 and PAI-05-022). J.C.G.-M. and L.P. acknowledge the receipt of fellowships from the Ministerio de Educación y Ciencia and Junta de Comunidades de Castilla-La Mancha.

[1] *The Photosynthetic Reaction Center* (Eds.: J. Deisenhofer, J. R. Norris), Academic Press, **1993**.
[2] T. Brixner, J. Stenger, H. M. Vaswani, M. Cho, R. E. Blankenship, G. R. Fleming, *Nature* **2005**, *434*, 625–628.

  

[3] a) C. J. Brabec, N. S. Sariciftci, J. C. Hummelen, *Adv. Funct. Mater.* **2001**, *11*, 15–26; b) F. J. Wudl, *J. Mater. Chem.* **2002**, *12*, 1959–1963; c) J.-F. Nierengarten, *Solar Energy Mater. & Solar Cells* **2004**, *83*, 187–199.
[4] D. Gust, T. A. Moore, A. L. Moore, *Acc. Chem. Res.* **2001**, *34*, 40–48.
[5] a) M.-S. Choi, T. Yamazaki, I. Yamazaki, T. Aida, *Angew. Chem.* **2004**, *116*, 152–160; *Angew. Chem. Int. Ed.* **2004**, *43*, 150–158; b) V. Balzani, A. Juris, *Coord. Chem. Rev.* **2001**, *211*, 97–115; c) A. Adronov, J. M. J. Fréchet, *Chem. Commun.* **2000**, 1701–1710; d) S. L. Gilat, A. Adronov, J. M. J. Fréchet, *Angew. Chem.* **1999**, *111*, 1519–1524; *Angew. Chem. Int. Ed.* **1999**, *38*, 1422–1427; e) V. Balzani, S. Campagna, G. Denti, A. Juris, S. Serroni, M. Venturi, *Acc. Chem. Res.* **1998**, *31*, 26–34; f) D.-L. Jiang, T. Aida, *Nature* **1997**, *388*, 454–456; g) G. M. Stewart, M. A. Fox, *J. Am. Chem. Soc.* **1996**, *118*, 4354–4360.
[6] J.-F. Nierengarten, *Top. Curr. Chem.* **2003**, *228*, 87–110.
[7] a) N. Armaroli, F. Barigelleti, P. Ceroni, J.-F. Eckert, J.-F. Nicoud, J.-F. Nierengarten, *Chem. Commun.* **2000**, 599–600; b) J.-F. Eckert, J.-F. Nicoud, J.-F. Nierengarten, S.-G. Liu, L. Echegoyen, F. Barigelleti, N. Armaroli, L. Ouali, V. Krasnikov, G. Hadziioannou, *J. Am. Chem. Soc.* **2000**, *122*, 7467–7479; c) N. Armaroli, G. Accorsi, J.-P. Gisselbrecht, M. Gross, V. Krasnikov, D. Tsamouras, G. Hadziioannou, M. J. Gómez-Escalonilla, F. Langa, J.-F. Eckert, J.-F. Nierengarten, *J. Mater. Chem.* **2002**, *12*, 2077–2087; d) G. Accorsi, N. Armaroli, J.-F. Eckert, J.-F. Nierengarten, *Tetrahedron Lett.* **2002**, *43*, 65–68.
[8] F. Langa, M. J. Gómez-Escalonilla, E. Díez-Barra, J. C. García-Martinez, A. de la Hoz, J. Rodríguez-López, A. González-Cortés, V. López-Arza, *Tetrahedron Lett.* **2001**, *42*, 3435–3438.
[9] D. M. Guldi, A. Swartz, C. Luo, R. Gómez, J. L. Segura, N. Martín, *J. Am. Chem. Soc.* **2002**, *124*, 10875–10886.
[10] a) G. R. Newcome, E. He, C. N. Moorefield, *Chem. Rev.* **1999**, *99*, 1689–1746; b) J. Palomero, J. A. Mata, F. González, E. Peris, *New J. Chem.* **2002**, *26*, 291–297, and references therein.
[11] S. Barlow, S. R. Marder, *Chem. Commun.* **2000**, 1555–1562.
[12] a) F. D'Souza, M. E. Zandler, P. M. Smith, G. R. Deviprasad, K. Arkady, M. Fujitsuka, O. Ito, *J. Phys. Chem. A* **2002**, *106*, 649–656; b) M. E. Zandler, P. M. Smith, M. Fujitsuka, O. Ito, F. D'Souza, *J. Org. Chem.* **2002**, *67*, 9122–9129.
[13] E. Díez-Barra, J. C. García-Martínez, S. Merino, R. del Rey, J. Rodríguez-López, P. Sánchez-Verdú, J. Tejeda, *J. Org. Chem.* **2001**, *66*, 5664–5670.
[14] The synthesis of ferrocene dendron **3** has been previously reported using a different approach based on a Heck coupling; see ref. [10b].
[15] M. Prato, M. Maggini, *Acc. Chem. Res.* **1998**, *31*, 519–526.
[16] M. Prato, M. Maggini, C. Giacometti, G. Scorrano, G. Sandona, G. Farnia, *Tetrahedron* **1996**, *52*, 5221–5234.
[17] L. Echegoyen, L. E. Echegoyen, *Acc. Chem. Res.* **1998**, *31*, 593–601.
[18] S. M. Batterjee, M. I. Marzouk, M. E. Aazab, M. A. El-Hashash, *Appl. Organomet. Chem.* **2003**, *17*, 291–297.
[19] A. Gouloumis, S.-G. Liu, A. Sastre, P. Vázquez, L. Echegoyen, T. Torres, *Chem. Eur. J.* **2000**, *6*, 3600–3607.
[20] D. González-Rodríguez, T. Torres, D. M. Guldi, J. Rivera, L. Echegoyen, *Org. Lett.* **2002**, *4*, 335–338.
[21] a) Y. Nakamura, T. Minowa, S. Tobita, H. Shizuka, J. Nishimura, *J. Chem. Soc. Perkin Trans. 2* **1995**, 2351–2357; b) J. Llacay, J. Veciana, J. Vidal-Gancedo, J. L. Bourdelande, R. González-Moreno, C. Rovira, *J. Org. Chem.* **1998**, *63*, 5201–5210; c) R. Fong II, D. I. Schuster, S. R. Wilson, *Org. Lett.* **1999**, *1*, 729–732; d) S.-G. Liu, L. Shu, J. Rivera, H. Liu, J.-M. Raimundo, J. Roncali, A. Gorgues, L. Echegoyen, *J. Org. Chem.* **1999**, *64*, 4884–4886; e) T. Ohno, K. Moriwaki, T. Miyata, *J. Org. Chem.* **2001**, *66*, 3397–3401.
[22] Y. Matsubara, H. Tada, S. Nagase, Z.-i. Yoshida, *J. Org. Chem.* **1995**, *60*, 5372–5373.
[23] R. M. Williams, J. M. Zwier, J. W. Verhoeven, *J. Am. Chem. Soc.* **1995**, *117*, 4093–4099.
[24] a) S. P. Sibley, S. M. Argentine, A. H. Francis, *Chem. Phys. Lett.* **1992**, *188*, 187–193; b) D. Kim, M. Lee, Y. D. Suh, S. K. Kim, *J. Am. Chem. Soc.* **1992**, *114*, 4429–4430; c) Y. P. Sun, P. Wang, N. B. Hamilton, *J. Am. Chem. Soc.* **1993**, *115*, 6378–6381.
[25] P. J. Bracher, D. I. Schuster in *Fullerenes: From Synthesis to Optoelectronic Properties* (Eds.: D. M. Guldi, N. Martín), Kluwer Academic Publishers, Dordrecht, **2002**, pp. 163–212.
[26] M. Fujitsuka, O. Ito, H. Imahori, K. Yamada, H. Yamada, Y. Sakata, *Chem. Lett.* **1999**, *28*, 721–722.
[27] S. Fukuzumi, H. Imahori, H. Yamada, M. E. El-Khouly, M. Fujitsuka, O. Ito, D. M. Guldi, *J. Am. Chem. Soc.* **2001**, *123*, 2571–2575.
[28] C. Luo, M. Fujitsuka, A. Watanabe, O. Ito, L. Gan, Y. Huang, C.-H. Huang, *J. Chem. Soc. Faraday Trans.* **1998**, *94*, 527–532.
[29] M. Fujitsuka, N. Tsuboya, R. Hamasaki, M. Ito, S. Onodera, O. Ito, Y. Yamamoto, *J. Phys. Chem. A* **2003**, *107*, 1452–1458.
[30] T. Yamashiro, Y. Aso, T. Otsubo, H. Tang, Y. Harima, K. Yamashita, *Chem. Lett.* **1999**, *28*, 443–444.
[31] A. Weller, *Z. Phys. Chem. (Muenchen Ger.)* **1982**, *133*, 93–98.
[32] MM+ force field as implemented in Hyperchem 5.0.
[33] M. Fujitsuka, O. Ito, T. Yamashiro, Y. Aso, T. Otsubo, *J. Phys. Chem. A* **2000**, *104*, 4876–4881.
[34] R. A. Marcus, *Angew. Chem.* **1993**, *105*, 1161–1172; *Angew. Chem. Int. Ed. Engl.* **1993**, *32*, 1111–1121.
[35] D. M. Guldi in *Fullerenes: From Synthesis to Optoelectronic Properties* (Eds.: D. M. Guldi, N. Martín), Kluwer Academic Press, Dordrecht, **2002**, pp. 237–266.
[36] F. D'Souza, S. Gadde, M. E. Zandler, K. Arkady, M. E. El-Khouly, M. Fujitsuka, O. Ito, *J. Phys. Chem. A* **2002**, *106*, 12393–12404.

Received: February 14, 2006
Published online: April 27, 2006

  